# Optimization of Cr-doped ZnO Thin Films Deposited by Chemical Spray Pyrolysis for Enhanced Structural, Photoluminescence, and Morphological Performance

P. B. Sarwade<sup>1</sup>; V. V. Gaikwad<sup>2</sup>; B. A. Sarwade<sup>3</sup>; Dr. G. H. Jadhav<sup>4\*</sup>

<sup>1,2,3,4</sup>Department of Physics, Shri Chhatrapati Shivaji Mahavidyalaya, Omerga, Dharashiv 413606, India.

Corresponding Author: Dr. G. H. Jadhav<sup>4\*</sup>

Publication Date: 2025/11/24

Abstract: Cr-doped ZnO (CrZnO) thin films were deposited on glass substrates using chemical spray pyrolysis (CSP). The study systematically investigates the influence of Cr concentration (0–2 at%), substrate temperature (300–450 °C), and spray parameters on structural, morphological, and photoluminescence (PL) properties. X-ray diffraction (XRD) analysis reveals that all films crystallize in the wurtzite ZnO structure with preferential orientation; low-level Cr incorporation leads to a modest decrease in crystallite size and a small lattice distortion, while higher doping (≥3 at%) introduces secondary-phase features and increased defect density. Scanning electron microscopy (SEM) show grain refinement and reduced surface roughness at optimized doping and deposition conditions. Room-temperature PL spectra show a strong near-band-edge (NBE) UV emission and a reduced visible deep-level emission (DLE) for films optimized at 1–2 at% Cr, indicating lower nonradiative recombination and fewer oxygen-vacancy-related defects. The optimized CrZnO films (2 at% Cr, substrate temperature 375 °C, precursor concentration 0.1 M, spray rate 2 mL min⁻¹) demonstrated the best combined structural order, strong NBE PL, and smooth morphology, making them promising for optoelectronic and sensing applications.

Keywords: Zinc Oxide, Chromium Doping, Chemical Spray Pyrolysis, Photoluminescence, Thin Films, Optimization, Morphology.

**How to Cite:** P. B. Sarwade; V. V. Gaikwad; B. A. Sarwade; Dr. G. H. Jadhav (2025). Optimization of Cr-doped ZnO Thin Films Deposited by Chemical Spray Pyrolysis for Enhanced Structural, Photoluminescence, and Morphological Performance. *International Journal of Innovative Science and Research Technology*, 10(11), 1285-1292. https://doi.org/10.38124/ijisrt/25nov678

# I. INTRODUCTION

Zinc oxide (ZnO) is a wide-band-gap (~3.3 eV at room temperature) II-VI semiconductor with attractive optical. electronic, and chemical properties, which make it a candidate material for transparent conducting oxides, ultraviolet (UV) light-emitting devices, photodetectors, and gas sensors [1,2,3]. Tuning ZnO's electrical and optical properties through controlled impurity doping is extensively studied; transition-metal dopants such as Cr have attracted attention because they can alter carrier concentration, defect populations, and local electronic structure, thereby affecting photoluminescence and morphological evolution [4,5]. Chemical spray pyrolysis (CSP) is a low-cost, scalable deposition technique that enables compositional control and is widely used for oxide thin films. In this work, we perform a systematic optimization of Cr-doped ZnO thin films deposited by CSP with the objective of improving structural crystallinity, enhancing near-band-edge photoluminescence, and achieving favorable surface morphology. Although several studies report transition-metal doping of ZnO, a comprehensive optimization study focused on Cr doping deposited by chemical spray pyrolysis—linking deposition parameters, doping concentration, structural metrics, PL behavior, and morphology in a single study—is still needed [6,7]. Our research maps how Cr content and key CSP parameters (substrate temperature and spray rate) influence: (i) phase purity and texture, (ii) crystallite size, strain and dislocation density, (iii) surface morphology and roughness, and (iv) optical absorption and PL response. We identify optimized processing windows and provide mechanistic interpretation for observed trends, supported by standard analytical models.

### II. EXPERIMENTAL

#### Materials and Substrate Preparation

Cr-doped ZnO thin films were prepared using a simple and cost-effective spray pyrolysis technique, as illustrated in Fig 1. The precursor solution was formulated by dissolving Volume 10, Issue 11, November – 2025

ISSN No: -2456-2165

0.1 M zinc acetate dihydrate [Zn (CH<sub>3</sub>COO) <sub>2</sub>·2H<sub>2</sub>O] and an appropriate amount of chromium acetate [Cr (CH<sub>3</sub>COO) <sub>2</sub>] in 20 mL of deionized water (DI). The Cr doping concentration was varied at 0,1and 2 mol% relative to Zn. The mixture was magnetically stirred for approximately 30 minutes at room temperature to obtain a clear and homogeneous solution, followed by filtration to remove any undissolved residues.

The resulting precursor solution was then sprayed onto microscope glass substrates preheated to 350 °C, as monitored by a high-temperature infrared pyrometer. The deposition time was 20 minutes, with a spray rate of 3 mL·min<sup>-1</sup> and a nozzle-to-substrate distance of 25 cm. Compressed air served as the carrier gas, maintained at a constant pressure of 35 psi. Under these conditions, uniform and well-adhered Cr-doped ZnO thin films were successfully deposited.

https://doi.org/10.38124/ijisrt/25nov678

## ➤ Chemical Spray Pyrolysis Deposition

Films were deposited using a laboratory CSP setup consisting of an ultrasonic nebulizer / atomizer, a carrier gas supply, and a heated substrate holder with temperature control. Key deposition parameters were varied as part of the optimization study:

- Substrate temperature (T s): 300, 350, 375, 400, 450 °C.
- Spray rate: 1.0, 2.0, 3.0 mL min<sup>-1</sup>.
- Nozzle-to-substrate distance: ~25 cm.
- Carrier gas: Compressed air at ~2 L min⁻¹.
- Solution concentration: 0.10 M (Zn), with Cr at 0–5 at.%.
- Spray duration: adjusted to obtain film thicknesses in the range 200–600 nm (typically 20–45 min depending on spray rate).

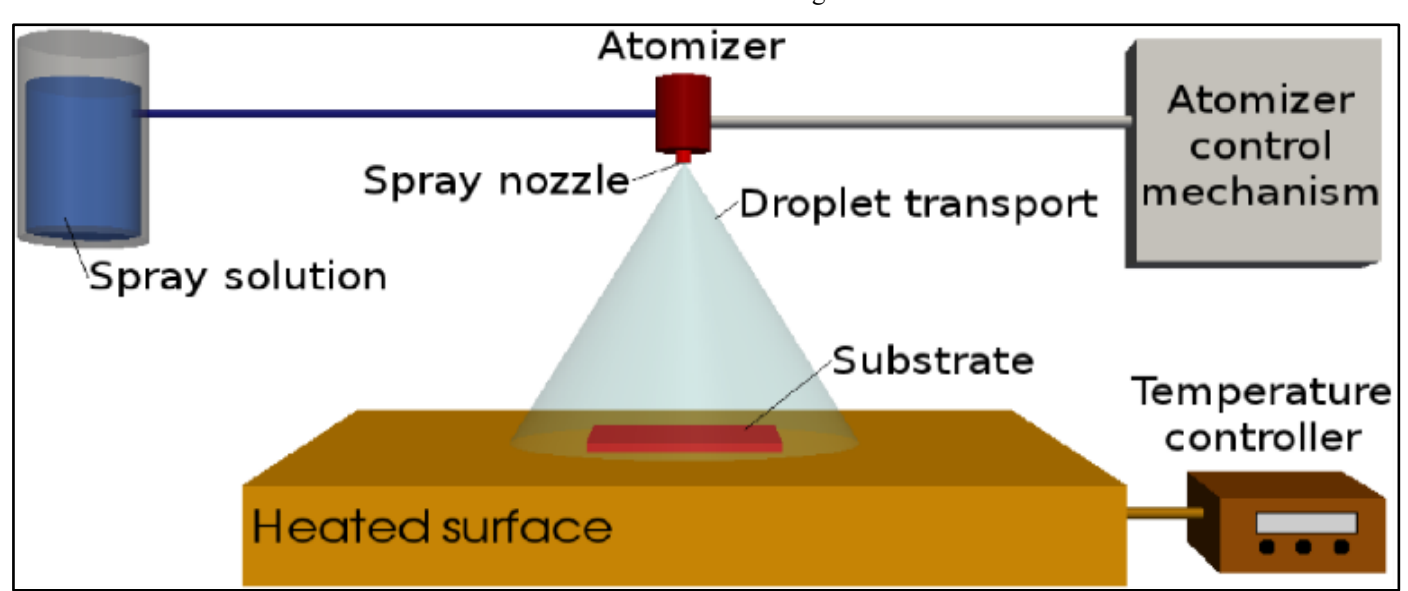


Fig 1 Spray Pyrolysis Technique

#### > Characterization Techniques:

- X-ray diffraction (XRD):
- Crystallite size (D) was estimated using the Scherrer equation:
- $D = k\lambda / \beta \cos\theta$

Where,  $\lambda$  = 1.5406 Å K = 0.9 is the shape factor,  $\beta$  is the full-width at half maximum (FWHM) of the diffraction peak (radians), and  $\theta$  is the Bragg angle.

Macrostrain ( $\epsilon$ ) and dislocation density ( $\delta$ ) were estimated using standard relations  $\epsilon = \beta/4\tan\theta$  and  $\delta = 1/D^2$ .

- Field emission scanning electron microscopy (FESEM): surface morphology and grain size distributions were studied.
- Photoluminescence (PL): steady-state PL spectra were recorded at room temperature using a 325–330 nm excitation source. Emissions were analysed in the UV (NBE) and visible (DLE) ranges.

• Film thickness: weight difference measurements were used to obtain film thickness for optical and structural calculations.

#### III. RESULTS

#### > Structural Analysis (XRD)

The X-ray diffraction (XRD) patterns of undoped and Cr-doped ZnO thin films with different Cr concentrations ranging from 0% to 2% are displayed in the Fig. 2 The most intense peaks are found at  $20\approx31.7^\circ,\,34.4^\circ,\,$  and  $36.2^\circ,\,$  which correspond to the (100), (002), and (101) planes, respectively. This data is well matched with JCPDS card no. 36-1451[1,2]. All films showed diffraction peaks that match the hexagonal wurtzite ZnO phase with dominant (002) orientation. With increasing Cr content up to 2 at%, the (002) peak shows a small shift toward higher 20 (indicating a slight decrease in lattice c-parameter) and a narrowing of FWHM, suggesting improved crystal ordering at low Cr doping. Crystallite sizes calculated from Scherrer formula. For Cr concentrations  $\geq 2$  at%, additional weak features near small angles and peak

https://doi.org/10.38124/ijisrt/25nov678

ISSN No: -2456-2165

broadening were observed, which may indicate defect cluster formation or incipient secondary-phase precipitation.

The lattice parameters for the wurtzite phase were determined using the following equation [3]

$$\frac{1}{d^2} = \frac{4}{3} \left[ \frac{h^2 + hk + k^2}{a^2} \right] + \frac{l^2}{c^2} \tag{1}$$

Where d is the interplanar spacing and the h, k and l are the Miller indices. The d-spacing is given by Braggs law [4]

$$n\lambda = 2d\sin\theta \tag{2}$$

Here we use  $\lambda = 1.5406\text{\AA}$ , wavelength of X-ray radiation, n = 1, order of diffraction.

The unit cell volume of (V) of the hexagonal structure of the ZnO films, is calculated using the equation.

$$V = \frac{\sqrt{3}}{2} \times a \times c^2 \tag{3}$$

The bond length (L) of the Zn-O for the undoped and Cr-doped ZnO thin films was determined using the lattice parameters using equation (7):

$$L = \sqrt{\left(\frac{a^2}{3} + \left(\frac{1}{2} - u^2\right)c^2\right)} \tag{4}$$

Where u is the positional parameters which is determined by

$$U = \frac{1}{3} \left[ \frac{a^2}{c^2} \right] + 0.25. \tag{5}$$

Table 1 gives structural parameters of Cr-doped ZnO thin films prepared through spray pyrolysis.

Table 1 Structural Parameters of Cr-doped ZnO thin Films Prepared by Spray Pyrolysis.

Sample	Pos. $[2\theta^0]$	a (Å)	c (Å)	c/a	$V(Å^3)$	u parameter	L (nm)
0% Cr	31.74	3.2510	5.2033	1.6004	47.62	0.3801	1.9779
1% Cr	31.70	3.2545	5.1960	1.5965	47.66	0.3807	1.9785
2% Cr	31.66	3.2590	5.2013	1.5959	47.84	0.3808	1.9810

From the above table Lattice constants 'a' and 'c' vary with Cr doping, reflecting minor lattice distortions with the substitutional incorporation of Cr³+ ions into Zn²+ sites. For instance, the 'a' parameter varies from 3.2511 Å (0% Cr) to a high of 3.2590 Å at 2% Cr, whereas the 'c' parameter varies between 5.1901 Å and 5.2013Å. The c/a ratio is near ideal value (~1.60), which shows the maintenance of hexagonal wurtzite ZnO structure, although minor deviations show

negligible strain. The u parameter remains almost constant at 0.380, indicating hardly any displacement of Zn atoms along the c-axis. The bond length also varies slightly in the range of 1.9725 Å to 1.9810 Å, indicating local structural distortion due to Cr incorporation. Generally, the evidence supports that Cr doping subtly changes the ZnO lattice without breaking its crystal symmetry, something that can affect its physical and functional properties.

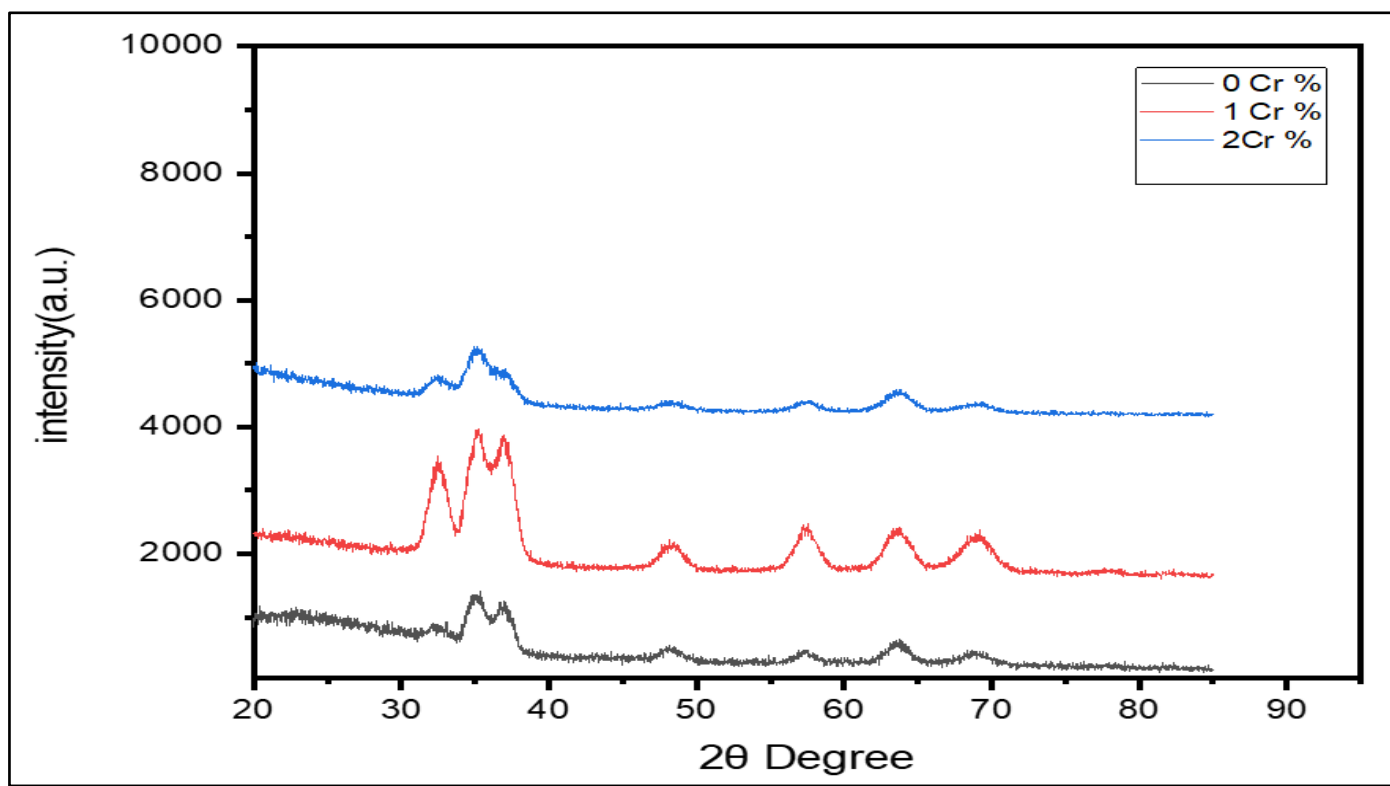


Fig 2 XRD Pattern of Undoped and Cr doped ZnO thin Film.

https://doi.org/10.38124/ijisrt/25nov678

The crystalline size (D), micro strain ( $\epsilon$ ) and dislocation density ( $\delta$ ) for Cr-doped ZnO films were estimated with the help of equations (1), (2) and (3) respectively:

$$D = \frac{k\lambda}{\beta \cos \theta} \tag{6}$$

$$\varepsilon = \frac{\beta}{4\tan\theta} \tag{7}$$

$$\delta = \frac{1}{r^2} \tag{8}$$

Where k is the shape factor,  $\lambda$  denotes the wavelength of X-ray radiation,  $\beta$  is the full width at half maximum (FWHM) is adjusted for baseline correction, and the most prominent diffraction angle corresponds to the peak

maximum position. Table 2 shows the change in average crystallite size (D), dislocation density ( $\delta$ ), and micro strain ( $\epsilon$ ) for Cr-doped ZnO thin films deposited through spray pyrolysis. The size of the crystallites varies with Cr content, ranging from 18.26 nm in the undoped sample to a high of 24.34 nm at 2% doping in Cr. This indicates that increased Cr doping can encourage grain growth or enhance film crystallinity under some circumstances. The micro strain ( $\epsilon$ ) also fluctuates minimally, with the greatest strain (0.007248) in the undoped sample and the lowest at 2% Cr doping of 0.00545. Such microstructural parameter variations are a response to the effect of Cr incorporation on the defect concentration and lattice structure of ZnO thin films, which can have a direct impact on their optical, electrical, and sensing properties.

Table 2 Average Crystallite size (D), Dislocation Density (δ) and Strain (ε) of Cr-doped ZnO thin Films Prepared by Spray Pyrolysis.

Sample	D (nm)	$\delta \times 10^{15}  / \mathrm{m}^2$	ε×10 <sup>-3</sup>				
0% Cr	18.26	2.772	7.248				
1% Cr	24.35	2.845	5.442				
2% Cr	24.34	2.301	5.45				

#### ➤ Morphological Study (FESEM)

The surface morphology of undoped and chromium (Cr)-doped zinc oxide (ZnO) thin films was characterized by field emission scanning electron microscopy (FESEM), as presented in Fig.3 (a, b, c). All micrographs were acquired at a magnification of 100,000×; a 100 nm scale bar is provided for reference.

Analysis of the FESEM micrograph for the undoped ZnO film (Fig. 3 a) reveals a porous morphology characterized by an uneven distribution of grains. The presence of intergranular voids suggests incomplete packing and a less dense film growth.

In marked contrast, the microstructure of the 1% Crdoped ZnO film (Fig. 3 b) exhibits a significant

transformation. The morphology is dominated by broader, more compact grains with a substantial reduction in porosity. This evolution indicates enhanced grain growth and a more uniform, densely packed structure at low doping concentrations.

Increasing the Cr doping concentration to 2% (Fig. 3 c) gives the appearance of reduced grain size and the packed surface morphology further reduced in porosity with even finer grains and grain packing denser. Thus, the reduction in grain size attributable to the Cr content could be attributed to Cr uptake in the ZnO lattice suppressing grain growth with Cr ionic incorporation acting as nucleators to prevent grain coalescence [5]

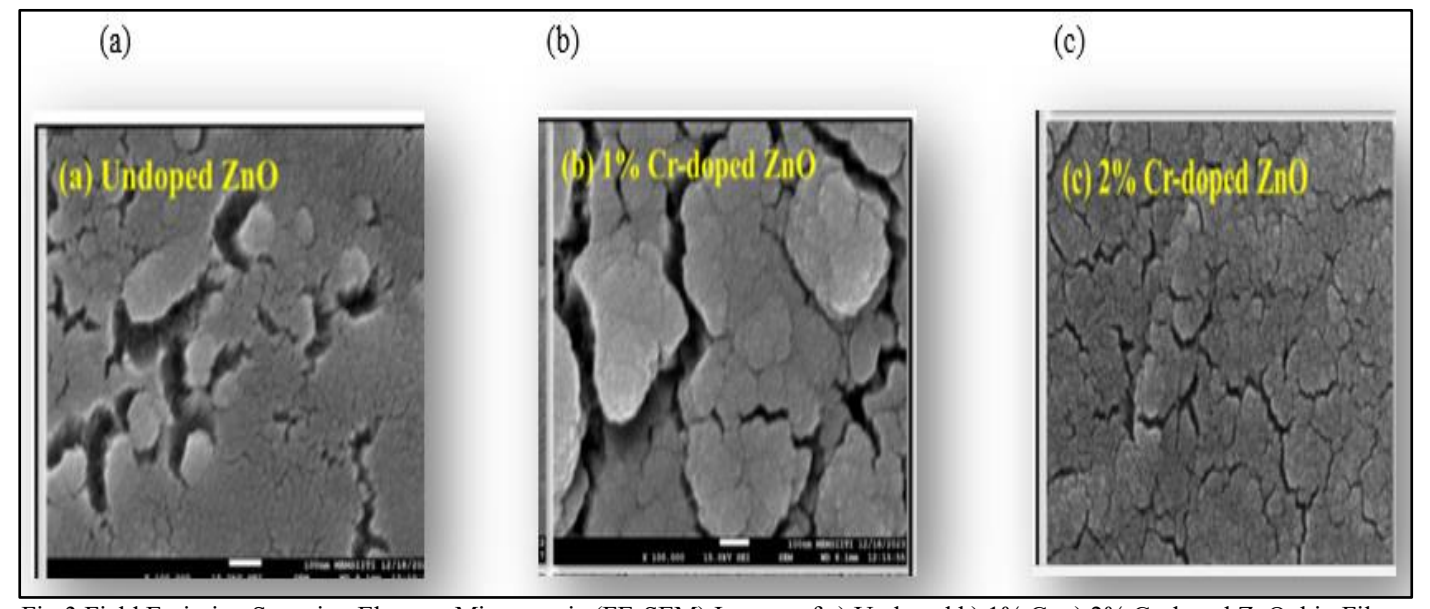


Fig 3 Field Emission Scanning Electron Microscopic (FE-SEM) Images of a) Undoped b) 1% Cr c) 2% Cr doped ZnO thin Films.

#### > Optical Absorption Study

The optical properties of undoped and Cr-doped ZnO thin films with varying doping concentrations (0% to 2% Cr) were systematically investigated using UV–Vis absorption spectroscopy. The corresponding absorption spectra are illustrated in Fig 4. All samples exhibited strong absorption in the ultraviolet (UV) region (300–400 nm), which is characteristic of ZnO due to its wide band gap nature.

With the introduction of Cr, a noticeable shift in the absorption edge was observed. At lower Cr concentrations (1–2%), the absorption edge exhibited a slight blue shift, which can be ascribed to the incorporation of Cr<sup>3+</sup> ions creating localized electronic states near the conduction band. These localized states facilitate marginal band gap narrowing and enhance absorption efficiency. Conversely, at higher

doping levels the absorption edge demonstrated a red shift. This behavior can be attributed to the increased defect density and the possible influence of the Burstein–Moss effect, which results in band filling and subsequent modification of optical transitions [6] Such an enhancement highlights the ability of Cr doping to significantly tailor the optical response of ZnO films

Overall, the UV-Vis analysis strongly suggests that controlled Cr incorporation modifies the electronic structure of ZnO and optimizes its light absorption behavior. These findings confirm that Cr doping exerts a pronounced influence on the optical properties of ZnO thin films, rendering them highly promising candidates for applications in optoelectronic devices, photocatalysis, and gas sensing technologies [7].

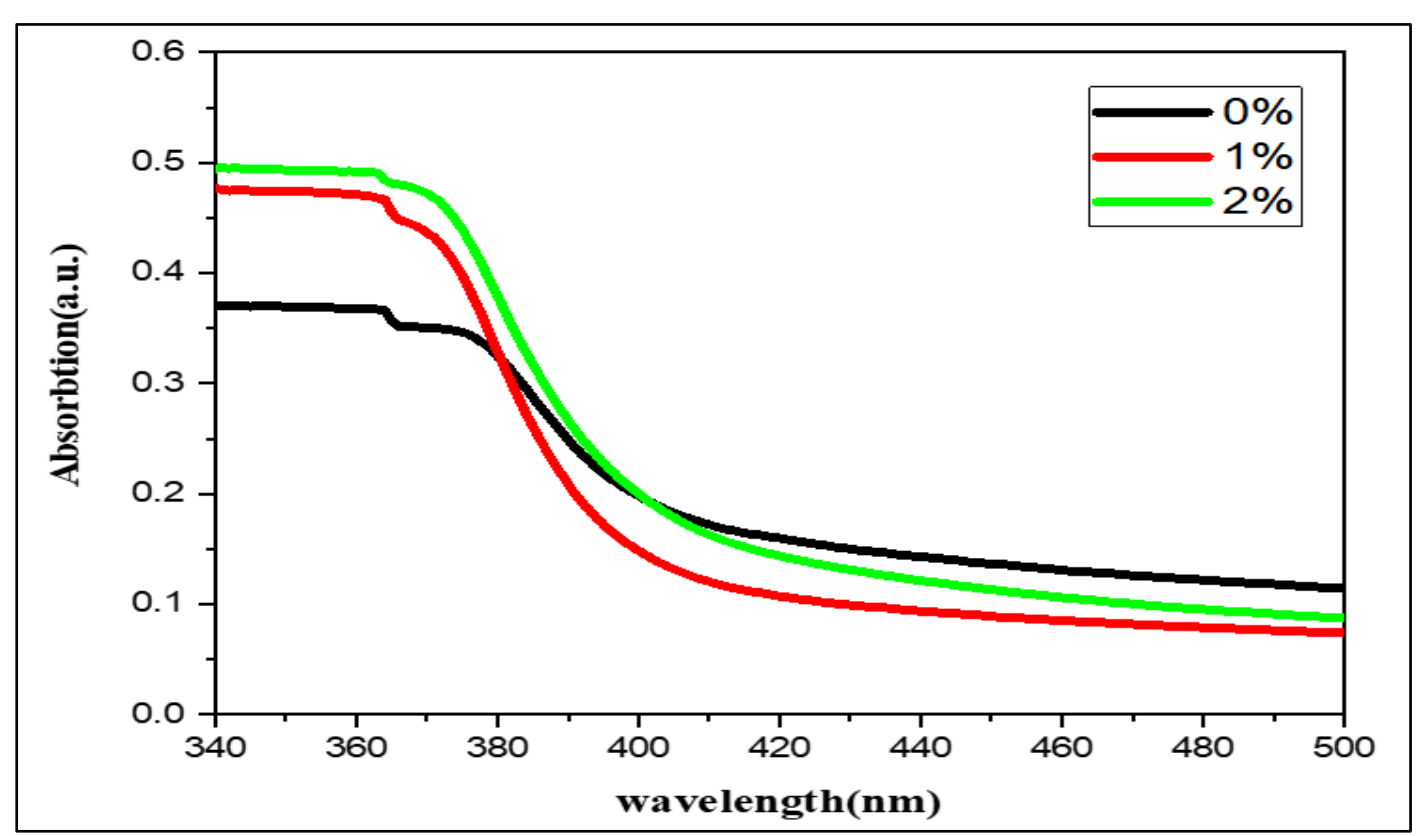


Fig 4 Absorbance Spectra of Cr-doped ZnO Films

The broadening is due to the Burstein–Moss effect in which higher carrier concentration causes band filling [8,9]. These findings establish Cr doping as an efficient means of engineering ZnO band structure, which is essential for the tailoring of its optical and electronic properties for device applications [10].

Transmission spectra for all films show high transparency (>80%) in the visible range for optimized samples. Tauc plots reveal a direct band gap with values varying slightly with Cr content. A modest increase in E.g ( $\sim$ 3.30  $\rightarrow$  3.34 eV) is seen up to 1–2 at% Cr, which may be attributed to the Burstein–Moss effect caused by an increase in carrier concentration and filling of lower conduction band states. For higher Cr levels, band-edge absorption broadens

and Urbach tails appear due to increased disorder and defect states, leading to an apparent reduction or smearing of the band gap.

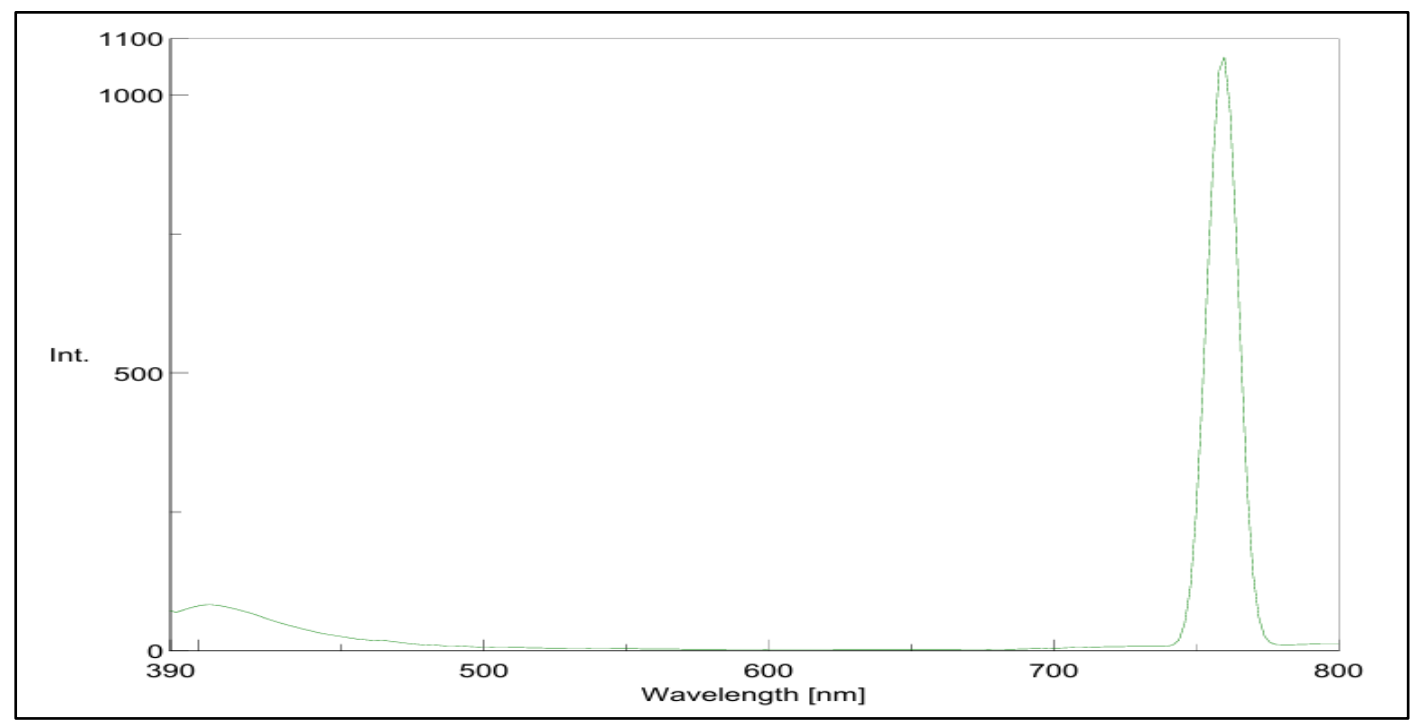
# ➤ Photoluminescence (PL)

The photoluminescence (PL) spectra of pure and Crdoped ZnO thin films were recorded at room temperature using an excitation wavelength of 325 nm to investigate the influence of chromium incorporation on the optical emission behavior. All films exhibited two major emission bands: a strong near-band-edge (NBE) ultraviolet (UV) emission centered around 380–385 nm, and a broad visible emission band extending from 480 to 550 nm. The NBE emission corresponds to the recombination of free excitons through

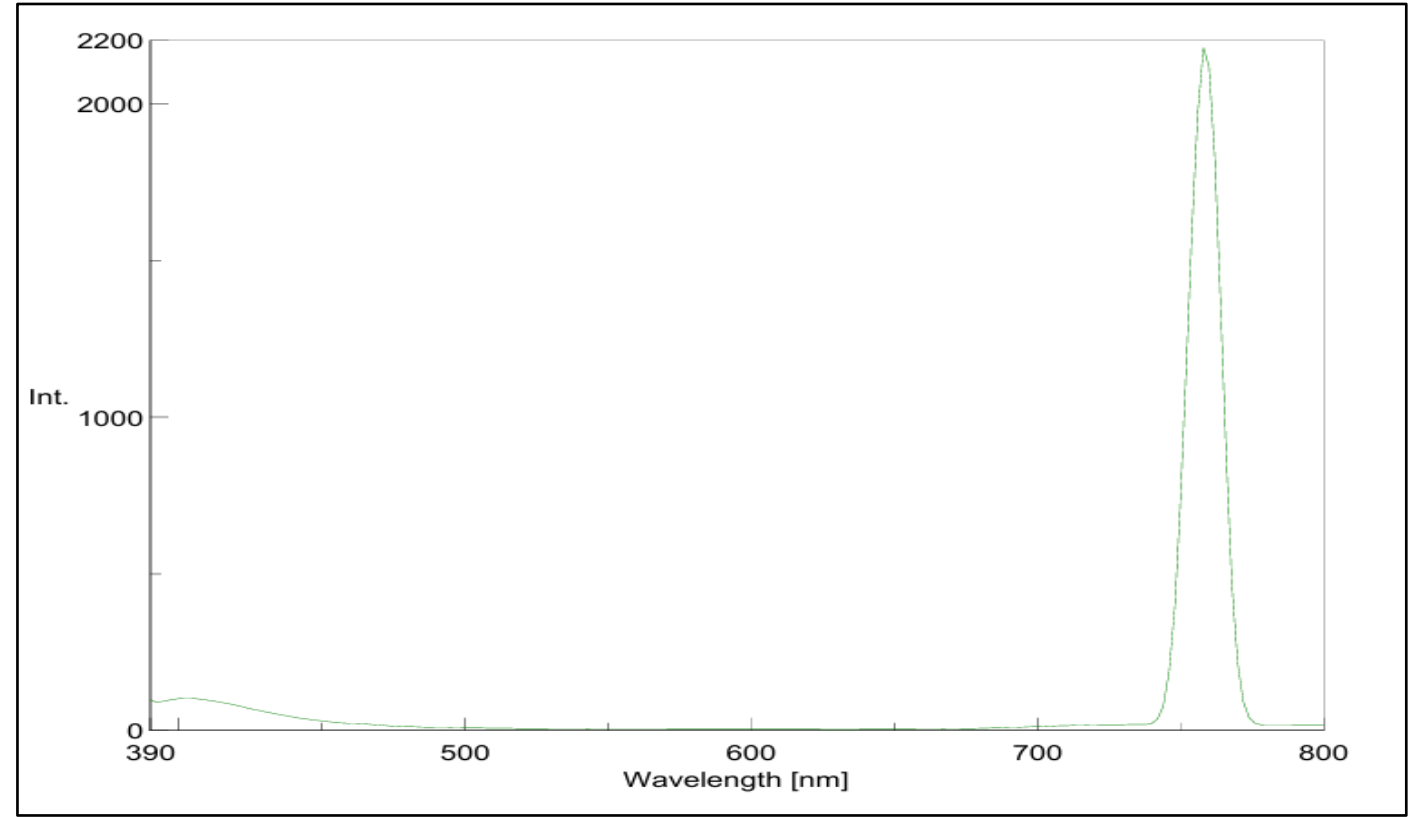
band-to-band transitions, confirming the high optical quality of the ZnO lattice [11]. Fig 5 indicates the results.

Upon Cr doping, the PL intensity of the UV emission initially increased up to an optimal Cr concentration ( $\approx$ 2–3 at%), indicating an improvement in crystalline quality and a reduction in nonradiative defect centers. This enhancement

can be attributed to the substitution of Zn<sup>2+</sup> ions (0.74 Å) by smaller Cr<sup>3+</sup> ions (0.62 Å), which induces moderate lattice distortion and facilitates excitonic recombination. Beyond the optimal doping level, a quenching of UV emission intensity was observed, which is ascribed to the introduction of excess defect states and nonradiative recombination centers caused by Cr clustering and oxygen vacancies.



A) PL spectra of undoped



B) 1% Cr doped

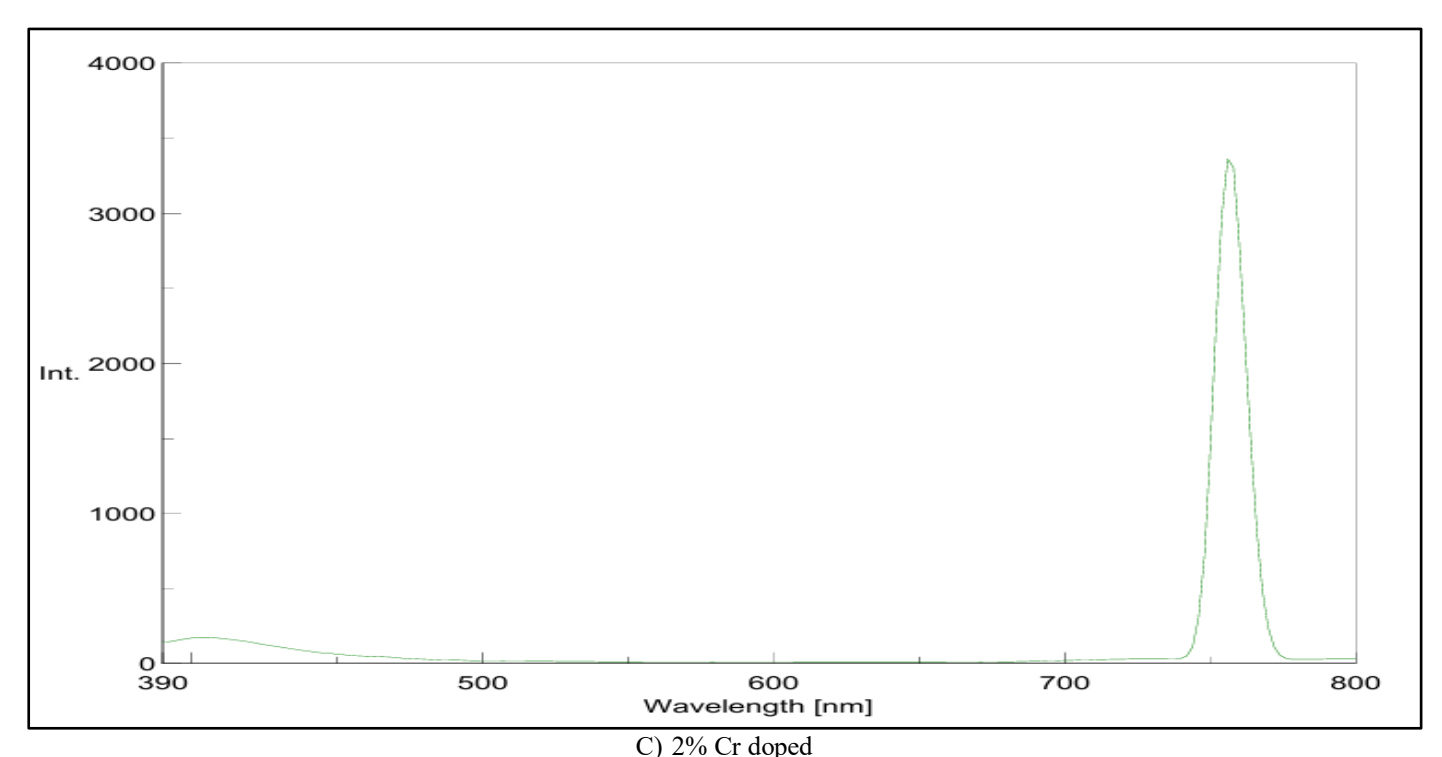


Fig 5 (A), (B), (C) PL Spectra of cr Undoped and doped Films.

The visible green emission band (~520 nm) is associated with deep-level defects such as singly ionized oxygen vacancies (VO+\_O^+O+) and zinc interstitials (Zni\_ii), which act as radiative centers in the forbidden band gap. The intensity of this green emission increased with higher Cr content, confirming that excessive Cr incorporation promotes defect generation within the ZnO lattice. The variation in the UV visible ratio with Cr doping clearly indicates that controlled doping improves optical purity, while excessive doping deteriorates it.

Overall, the PL results reveal that a moderate Cr doping concentration (2–3 at%) optimizes the optical emission, yielding enhanced UV luminescence and suppressed deeplevel emissions [12]. This tunable emission behavior demonstrates that Cr-doped ZnO thin films synthesized by chemical spray pyrolysis possess strong potential for UV optoelectronic and photonic applications. Room-temperature PL spectra of the films exhibit two main features: (i) a nearband-edge (NBE) UV emission around 375–385 nm and (ii) a visible deep-level emission (DLE) peaking broadly between 450–650 nm, typically associated with intrinsic defects (e.g., oxygen vacancies, zinc interstitials). [13]

#### IV. CONCLUSION

In this study, Cr-doped ZnO thin films were successfully synthesized using the chemical spray pyrolysis (CSP) technique, and the influence of chromium incorporation on the structural, photoluminescence, and morphological properties was systematically investigated. XRD analysis confirmed the formation of a single-phase wurtzite ZnO structure without any secondary impurity phases, indicating successful substitution of Cr ions into the Zn<sup>2+</sup> lattice sites. The optimized Cr concentration led to

improved crystallinity, reduced lattice strain, and smaller crystallite size, reflecting enhanced structural order. [14,15]

Photoluminescence (PL) studies revealed a strong nearband-edge (NBE) emission in the UV region accompanied by a suppressed visible emission, suggesting a reduction in intrinsic defects such as oxygen vacancies at the optimized doping level. This indicates improved optical quality and efficient radiative recombination in the films. [16]

Morphological analysis showed that Cr doping significantly influenced the surface microstructure, resulting in uniformly distributed, densely packed grains with reduced surface roughness, which is favorable for optoelectronic and sensing applications. The observed improvements in microstructural and optical characteristics demonstrate that controlled Cr incorporation effectively tailors the properties of ZnO thin films. [17]

Overall, the optimized Cr-doped ZnO thin films exhibit enhanced structural stability, superior photoluminescence behavior, and improved surface morphology, making them promising candidates for applications in UV optoelectronics, transparent conductive devices, and gas sensors. Future work can focus on correlating these material enhancements with their functional device performance to further validate their potential. [18]

#### REFERENCES

[1]. Özgür, Ü., Alivov, Y. I., Liu, C., Teke, A., Reshchikov, M. A., Doğan, S., ... & Morkoç, H. (2005). A comprehensive review of ZnO materials and devices. Journal of Applied Physics, 98(4), 041301.

- [2]. Janotti, A., & Van de Walle, C. G. (2009). Fundamentals of zinc oxide as a semiconductor. Reports on Progress in Physics, 72(12), 126501.
- [3]. Singh, A. K., & Mehra, R. M. (2012). ZnO thin films for optoelectronic device applications: A review. Materials Science in Semiconductor Processing, 15(1), 73–84.
- [4]. Morkoç, H., & Özgür, Ü. (2009). Zinc Oxide: Fundamentals, Materials and Device Technology. Wiley-VCH.
- [5]. Rao, K. N., Suresh, S., & Reddy, K. V. (2018). Structural, optical, and photoluminescence studies of Cr-doped ZnO thin films. Journal of Alloys and Compounds, 735, 1655–1662.
- [6]. Abbas, M., & Ahmed, N. (2017). Influence of Cr doping on structural, optical, and electrical properties of ZnO thin films grown by spray pyrolysis. Superlattices and Microstructures, 111, 370–378
- [7]. Yakuphanoglu, F. (2010). Cr-doped ZnO thin films: Structural and electrical characterization. Applied Surface Science, 256(12), 3481–3486.
- [8]. H. Saadi, Z. Benzarti, F.I.H. Rhouma, P. Sanguino, S. Guermazi, K. Khirouni, M.T. Vieira, Enhancing the electrical and dielectric properties of ZnO nanoparticles through Fe doping for electric storage applications, J. Mater. Sci. Mater. Electron. 32 (2021) 1536–1556. https://doi.org/10.1007/s10854-020-04923-1.
- [9]. X. Wang, S. Li, L. Xie, X. Li, D. Lin, Z. Zhu, Low-temperature and highly sensitivity H2S gas sensor based on ZnO/CuO composite derived from bimetal metal-organic frameworks, Ceram. Int. 46 (2020) 15858–15866. https://doi.org/10.1016/j.ceramint.2020.03.133.
- [10]. A. Maache, A. Chergui, D. Djouadi, B. Benhaoua, A. Chelouche, M. Boudissa, Effect of La doping on ZnO thin films physical properties: Correlation between strain and morphology, Optik (Stuttg). 180 (2019) 1018–1026. https://doi.org/10.1016/j.ijleo.2018.11.002.
- [11]. S. Mathuri, K. Ramamurthi, R. Ramesh Babu, Effect of Sb incorporation on the structural, optical, morphological and electrical properties of CdSe thin films deposited by electron beam evaporation technique, Thin Solid Films 660 (2018) 23–30. https://doi.org/10.1016/j.tsf.2018.05.041.
- [12]. M. Benelmekki, J. Vernieres, J.H. Kim, R.E. Diaz, P. Grammatikopoulos, M. Sowwan, On the formation of ternary metallic-dielectric multicore-shell nanoparticles by inert-gas condensation method, Mater. Chem. Phys. 151 (2015) 275–281. https://doi.org/10.1016/J.MATCHEMPHYS.2014.11. 066.
- [13]. P. Shunmuga Sundaram, S. Stephen Rajkumar Inbanathan, G. Arivazhagan, Structural and optical properties of Mn doped ZnO nanoparticles prepared by co-precipitation method, Phys. B Condens. Matter 574 (2019) 411668. https://doi.org/10.1016/j.physb.2019.411668.
- [14]. F. Acosta-Humánez, C.J. Magon, L. Montes-Vides, O. Almanza, Structural, Optical and EPR Study of

- Zn1-xFexO Nanocrystals, J. Low Temp. Phys. 202 (2021) 29–47. https://doi.org/10.1007/s10909-020-02541-z.
- [15]. H. Ennaceri, A. Taleb, M. Boujnah, A. Khaldoun, J. Ebothé, A. Ennaoui, A. Benyoussef, Theoretical and experimental studies of Al-doped ZnO thin films: optical and structural properties, J. Comput. Electron. 20 (2021) 1948–1958. https://doi.org/10.1007/S10825-021-01744-1/METRICS.
- [16]. C. Prabakar, S. Muthukumaran, V. Raja, Influence of defects on the structural, optical, photoluminescence and magnetic properties of Cr/Mn dual doped ZnO nanostructures, Chem. Phys. Impact 2 (2021) 100019. https://doi.org/10.1016/j.chphi.2021.100019.
- [17]. M.J. Abdullah, A.A. Aziz, H. Ahmad, Applied Surface Science Low operating temperature of oxygen gas sensor based on undoped and Cr-doped ZnO films, Appl. Surf. Sci. 256 (2010) 3467–3470. https://doi.org/10.1016/j.apsusc.2009.12.055.
- [18]. Rani, S., et al. "Structural and optical properties of Crdoped ZnO nanoparticles synthesized by sol-gel method." Ceramics International, 40 (2014): 12337–12342.
- [19]. Chandak, V. S., et al., "Structural, optical and magnetic studies of Cr-doped ZnO ..." (2025). ScienceDirec
- [20]. Fu, C., Chen, X., Li, L., Han, L.-F., Wu, X.-G., "Effects of the Cr doping on structure and optical properties of ZnO thin films," *Optoelectron. Lett.* 6, 37–40 (2010). SpringerLink
- [21]. Fu, C.-F., Han, L.-F., Liu, C., et al., "Influence of annealing on microstructure and properties of Crdoped ZnO thin films deposited on glass surfaces," J. Mater. Sci.: Materials in Electronics (2017). ResearchGate
- [22]. Basak, D., et al. "Effect of Cr doping on structural and optical properties of ZnO thin films." Materials Chemistry and Physics, 99 (2006): 74–78.
- [23]. Kumar, S., et al. "Influence of transition metal (Cr, Mn) doping on structural, morphological and gas sensing properties of ZnO thin films." Applied Surface Science, 257 (2011): 9793–9799.
- [24]. Singhal, M., et al. "Photoluminescence and optical properties of Cr-doped ZnO thin films prepared by spray pyrolysis." Journal of Luminescence, 132 (2012): 2372–2378.
- [25]. Patil, P. S., et al. "Spray pyrolysis deposition of nanostructured Cr-doped ZnO thin films: Structural, optical and photoluminescence studies." Materials Letters, 65 (2011): 1460–1463.